Poly(norepinephrine)-mediated Universal Surface Modification for Patterning Human Pluripotent Stem Cell Culture and Differentiation

Gyuhyung Jin[1,2,3,], Haoning Huang[2,4], Xiaoping Bao[1,2], Sean P. Palecek[3]*

[1] Davidson School of Chemical Engineering, Purdue University, West Lafayette, IN, 47907, USA

[2] Purdue University Institute for Cancer Research, West Lafayette, IN, 47907, USA

[3] Department of Chemical and Biological Engineering, University of Wisconsin Madison, WI, 53706, USA

[4] Department of Biological Sciences, Purdue University, West Lafayette, IN, 47907, USA

*Corresponding author: G.J., jin443@purdue.edu.

Abstract

Maintaining undifferentiated states of human pluripotent stem cells (hPSCs) is key to accomplishing successful hPSC research. Specific culture conditions, including hPSC-compatible substrates, are required for hPSC culture. Over the past two decades, substrates supporting hPSC self-renewal have evolved from undefined and xenogeneic protein components to chemically defined and xenogeneic-free materials. However, these synthetic substrates are often costly and complex to use, leading many laboratories to continue using simpler undefined extracellular matrix (ECM) protein mixtures. In this study, we present a method using poly(norepinephrine) (pNE) for surface modification to enhance the immobilization of ECM proteins on various substrates, including polydimethylsiloxane (PDMS) and ultra-low attachment (ULA) hydrogels, thereby supporting hPSC culture and maintenance of pluripotency. The pNE-mediated surface modification enables spatial patterning of ECM proteins on non-adhesive ULA surfaces, facilitating tunable macroscopic cell patterning. This approach improves hPSC attachment and growth and allows for cell patterning to study the effects of anisotropic environments on hPSC fate. Our findings demonstrate the versatility and simplicity of pNE-mediated surface modification for improving hPSC culture and spatially controlled differentiation into endothelial cells and cardiomyocytes on previously non-amenable substrates, providing a valuable tool for tissue engineering and regenerative medicine applications.

Keywords: Human Pluripotent Stem Cell, Surface Modification, Cell Patterning

1. Introduction

Human pluripotent stem cell (hPSC) research has made significant progress in many fields such as human developmental studies, disease modeling, drug development, and cell therapies. A key aspect of this progress is the ability to maintain hPSCs in a long-term and stable undifferentiated and self-renewing manner. Maintaining hPSCs in their undifferentiated state requires appropriate culture conditions, including specific culture media and extracellular matrix (ECM) components[1]. Over the past two decades, substrates for supporting hPSC self-renewal have evolved from undefined and xenogeneic to chemically-defined and xenogeneic-free components[2]. Initially, mouse embryonic fibroblasts were used as feeder layers for human embryonic stem cell (hESC) culture[3]. This was followed by the use of Matrigel, an ECM derived from the Engelbreth–Holm–Swarm (EHS) mouse tumor, for feeder-free growth of hESCs[4]. Later, more defined extracellular proteins like vitronectin[5] and laminin[6] were introduced for hPSC culture. Recently, various synthetic substrates, including peptides and polymers, have been developed for well-defined, xenogeneic-free hPSC culture[7–11]. However, these synthetic substrates are often expensive and require complex coating processes[12]. Consequently, many laboratories still use simpler ECM protein mixtures like Matrigel for substrate preparation. While these substrates are mainly used for two-dimensional (2D) hPSC culture on tissue culture-treated polystyrene surfaces, there is an increasing need for three-dimensional (3D) hPSC culture to more accurately mimic the natural ECM microenvironment.

Protein-based ECM coating primarily relies on simple adsorption of the matrix onto a substrate[12]. While conventional tissue culture plates or glass generally support protein adsorption, the ability of other materials, such as polymers or hydrogels, to support protein adsorption varies greatly

based on their physical properties, including hydrophobicity and electric charge. These properties may require additional surface modifications for significant protein adsorption. For example, oxidizing carbon nanotubes can support the coating of Geltrex, which contains ECM proteins from the murine EHS tumor, to test the effects of surface roughness and mechanical stiffness on hPSC fate. When using scaffolds to recapitulate the structural characteristics of natural ECM or for three-dimensional hPSC culture and differentiation, substrates either need to be composed of natural ECM components[13–15] or require modification[16–18] to support hPSC culture.

Inspired by the composition of mussel-adhesive proteins rich in 3,4-dihydroxy-L-phenylalanine (DOPA) and lysine, catecholamines such as dopamine and norepinephrine (NE) have been widely used as versatile coating materials for substrate-independent surface modification[19,20]. In addition to their function as neurotransmitters, these catecholamines can be oxidized, forming poly(catecholamine) through covalent polymerization and physical self-assembly. This process produces a thin (~100 nm thick) film on the target substrate[21,22]. This poly(catecholamine) layer allows for the immobilization of bioactive molecules containing thiols or primary amines via covalent conjugation to the quinone group in the polymerized layer[23]. Due to its versatility and simplicity, poly(catecholamine)-mediated surface modification has been used to covalently immobilize ECM proteins on various substrates such as metals[24,25] and polymers[26,27] to support cell attachment and culture. This approach has also been used to modify substrates with vitronectin peptides[28–30], RGD-containing peptides[31], and collagen[32] to support hPSC culture.

In this study, we demonstrate that poly(norepinephrine) (pNE)-mediated surface modification enhances the immobilization of ECM proteins, particularly on polydimethylsiloxane (PDMS) and superhydrophilic hydrogel layers (Ultra-Low Attachment (ULA) surfaces), to support hPSC culture. Importantly, we achieved spatial patterning of pNE coating on a non-adhesive ULA

surface using PDMS stencil masks, enabling ECM protein immobilization only on the patterned areas and thus allowing tunable cell patterning. Spatial cell fate specification is critical during development, yet it is difficult to achieve spatial control over conventional *in vitro* cell culture and differentiation. This simple and versatile surface modification method facilitates not only the growth and differentiation of hPSCs on various substrates but also cell patterning to study the spatial effects of anisotropic patterning on hPSC colonies and their fate.

2. Materials and Methods

hPSC maintenance

H9 hESCs (WiCell) were maintained in mTeSR1 basal medium (STEMCELL Technologies, 85851) supplemented with 5X supplement (STEMCELL Technologies, 85852) or mTeSR™ Plus (STEMCELL Technologies, 100-0276) at 37 °C, 5% CO_2. When cells reached 70-80% confluency, they were passaged onto a Matrigel (Corning, 354230)-coated 6-well tissue culture (TC)-treated plate (Corning, 3516) with a split ratio of 1:9 using Versene (Gibco, 15040-066) or 5mM EDTA (5-6 min incubation at 37 °C). Matrigel-coated plates were prepared by diluting Matrigel in DMEM/F12 medium (Gibco, 11330-032) to a concentration of 0.08mg/ml, adding 1ml of Matrigel solution to each well of 6-well TC-treated plate, and incubating the plates at least 1 hour at 37 °C.

pNE coating and patterning

A 2 mg/ml NE solution was prepared by dissolving DL-Norepinephrine hydrochloride (Sigma, A7256) in 10 mM Tris buffer with pH 8.5. A 20 mg/ml sodium periodate solution was prepared by dissolving sodium periodate (Sigma, S1878) in distilled water. The NE and sodium periodate solutions were mixed at a 100:1 ratio (vol/vol) to induce oxidation of norepinephrine, and the

resulting mixture was immediately added to the substrates, ensuring surface coverage and subsequence surface modification. The substrates used included a 24-well TC-treated plate (Corning, 3524), a 12-well untreated plate (Corning, 351154), cover glass (FisherScientific, 12-545-80) placed in a 24-well TC-treated plate, PDMS (Electron Microscopy Sciences, 24236-10), and an Ultra-Low-Attachment (ULA) 24-well plate (Corning, 3473). Substrates with the NE + sodium periodate solution were incubated at room temperature for at least 10 minutes and washed with phosphate-buffered saline (PBS) (Gibco, 14190-144) at least three times to remove any residual solution. For patterning of pNE coating, PDMS masks were firmly attached to a ULA surface to ensure solution confinement. The NE + sodium periodate solution was placed as a 5 µl droplet or confined with PDMS stencil masks on a ULA plate to make sure the solution was in contact with only the patterned area. After 10 minutes of incubation at room temperature, the surface was washed with PBS at least three times to remove any residual solution. To make PDMS stencil masks, an in-house PDMS layer was prepared, cut, and punched with commercially available hole punches or cut with a razor blade to make a line pattern. Briefly, base elastomer and curing agent (Electron Microscopy Sciences, 24236-10) were mixed thoroughly at a 10:1 weight ratio, poured into a nonstick baking pan to cover the surface, degassed in a desiccator until bubbles were removed, cured in an oven for an hour at 100°C, and cooled for at least 24 hours at room temperature. The cured PDMS layer was detached from the pan and used to make stencil masks.

Cardiac progenitor cell (CPC) differentiation

CPCs were generated using the GSK inhibitor and Wnt inhibitor (GiWi) protocol[33]. Briefly, hPSCs were singularized using Accutase (Innovative Cell Technologies, AT104) (8 min incubation at 37°C), diluted in mTeSR1 (1:1 dilution), centrifuged (200 g, 5 min), and resuspended in mTeSR1 supplemented with 5 µM ROCK inhibitor Y-27632 (Selleckchem, S1049). Cells were

seeded at 250,000-400,000 cells/cm² on a Matrigel-coated 12-well TC-treated plate (Corning, 3513) (day -2). The next day, the medium was changed with fresh mTeSR1. On day 0, cells were treated with 7-10 μM CHIR99021 (Selleckchem, S1263) in RPMI1640 medium (Gibco, 11875-093) containing 1X B27 supplement minus insulin (A18956-01) (RPMI B27-) for 24 hours. On day 1, the medium was changed with fresh RPMI B27-. On day 3, cells were treated with 5 μM IWP2 (Tocris, 3533) in fresh RPMI B27-. On day 5, the medium was changed with fresh RPMI B27-. On day 6, cells were detached using Accutase (8 min incubation at 37°C) and cryopreserved in a cryopreservation medium (60% RPMI1640 medium containing 1X B27 supplement (17504-044) (RPMI B27+), 30% FBS (Peak Serum, PS-FB1), 10% dimethyl sulfoxide (DMSO) (Sigma, D2650), 5 μM Y-27632).

hPSC and CPC culture on pNE-modified substrate

The pNE-modified substrate was incubated with 0.08 mg/ml Matrigel in DMEM/F12 for at least 1 hour at 37°C before cell seeding. hPSCs were singularized using Accutase (8 min incubation at 37°C), diluted in mTeSR1 (1:1 dilution), centrifuged (200 g, 5 min), resuspended in mTeSR1 supplemented with 5 μM ROCK inhibitor Y-27632 (Selleckchem, S1049) and 1X Penicillin-Streptomycin (Gibco, 15140-122), and seeded at 20,000 or 200,000 cells/cm² on the Matrigel-coated substrate. The medium was changed with fresh mTeSR1 daily until analysis. Cryopreserved CPCs were thawed and seeded at 150,000-250,000 cells/cm² on the Matrigel-coated substrate. The medium was changed with fresh RPMI 27+ daily until analysis.

Patterned differentiation of hPSCs

hPSCs were plated on the pNE-modified substrate as described previously. Once they reached 80-90% confluency on the patterned substrate, the medium was changed to DMEM (Gibco, 11965-092) containing 100 μg/mL ascorbic acid and 6 μM CHIR99021 (day 0). On day 1, the medium

was changed to Advanced DMEM/F12 (Gibco 11320-033) containing 2.5 mM GlutaMAX and 60 μg/mL ascorbic acid (LaSR medium). The cells were immunostained for BRACHYURY and E-CADHERIN on day 2. For endothelial cell differentiation, the medium was changed to LaSR medium containing 50 ng/mL VEGF on days 2 and 3. The cells were immunostained for CD34 and CD31 on day 4. For patterned cardiomyocyte differentiation, a modified version of GiWi protocol was used. Briefly, hPSCs were singularized and plated as described previously for CPC differentiation. On day 0, cells were treated with 6 μM CHIR99021 in RBL medium for 48 hours. On day 2, cells were treated with 2 μM Wnt C-59 (Cayman Chemical, 16644) in fresh RBL medium. On day 4, the medium was changed with fresh RBL medium. On day 7 and every three days afterwards, the medium was changed with fresh RPMI 27+ until analysis.

Fluorescence staining

For laminin staining, the Matrigel-coated substrate was incubated in 4% paraformaldehyde (Electron Microscopy Sciences, 15710-S) in PBS for 15 minutes at room temperature, washed with PBS three times, and incubated in diluted anti-laminin antibody (ThermoFisher, PA1-16730, 1:5000) in 5% nonfat dry milk (Santa Cruz Biotechnology, sc-2324) PBS overnight at 4°C. The substrate was then washed with PBS three times and incubated in diluted chicken anti-rabbit IgG Alexa Fluor 488 (Invitrogen, A21441, 1:1000) in 5% nonfat dry milk PBS for 30 minutes at room temperature. After secondary antibody staining, the substrate was washed with PBS three times and analyzed under a fluorescence microscope. Live-dead cell staining was performed using a live-dead cell staining kit (BioVision, K501). All other staining followed a similar method. Cells were fixed in 4% paraformaldehyde in PBS for 15 minutes at room temperature, washed with PBS three times, and incubated in diluted antibody (anti-cTnT, BD Bioscience 564766 or ThermoFisher, MS-295-P1, 1:500/1:200; anti-sarcomeric alpha actinin, Invitrogen MA1-22863, 1:100; anti-

Brachyury, R&D Systems AF2085, 1:100; Alexa Fluor® 647-anti-E-cadherin, BD Bioscience 563571, 1:100; FITC-anti-CD34, Miltenyi Biotec, 130-113-178, 1:100; APC-anti-CD31, Miltenyi Biotec, 130-110-670, 1:100; anti-OCT4, Cell Signaling Technology 75463, 1:200; anti-NANOG, Cell Signaling Technology 3580, 1:800) in 5% nonfat dry milk (Santa Cruz Biotechnology, sc-2324)/0.4% Triton X-100 (Fisher Scientific, BP151-500) PBS overnight at 4°C. The cells were then washed with PBS three times. For unconjugated antibodies, the cells were incubated in diluted secondary antibody (goat anti-mouse IgG1 Alexa Fluor 488, Invitrogen, A21121, 1:1000; chicken anti-goat IgG1 Alexa Fluor 488, Invitrogen, A21467, 1:1000) in 5% nonfat dry milk/0.4% Triton X-100 PBS for 30 minutes at room temperature. The cells were then washed with PBS three times, incubated in 2 μg/ml Hoechst 33342 (Thermofisher, H3570) diluted in PBS for 5 minutes at room temperature, washed with PBS twice, and analyzed under a fluorescence microscope.

Flow cytometry

For flow cytometry analysis, cells were harvested by using Accutase (8 min, at 37°C) or 0.25% Trypsin/EDTA (Gibco, 25200072) (5 min at 37°C). The collected cells were centrifuged at 200 g for 5 min and then fixed in 1% PFA diluted in PBS for 20 min at room temperature, followed by another centrifugation step. After centrifugation, supernatant was carefully removed, and the pelleted cells were permeabilized in 90% methanol in -20°C overnight. The cells were washed with 2 ml of PBS containing 2.5% bovine serum albumin (BSA) by centrifugation and removing supernatant three times. Next, cells were incubated overnight at 4°C in 100 μl of diluted antibodies (anti-cTnT, ThermoFisher, MS-295-P1, 1:200; anti-Brachyury, R&D Systems AF2085, 1:100; Alexa Fluor® 647-anti-E-cadherin, BD Bioscience 563571, 1:100; FITC-anti-CD34, Miltenyi Biotec, 130-113-178, 1:100; APC-anti-CD31, Miltenyi Biotec, 130-110-670, 1:100; anti-OCT4, Cell Signaling Technology 75463, 1:100; anti-NANOG, Cell Signaling Technology 3580, 1:400)

in PBS containing 2.5% BSA and 0.1% Triton X-100. On the following day, the cells were washed once with PBS containing 2.5% BSA and 0.1% Triton X-100, resuspended in PBS containing 2.5% BSA and 0.1% Triton X-100 and diluted secondary antibodies (Goat anti-Mouse IgG1 Alexa Fluor™ 488, Invitrogen, A-21121, 1:1000; Chicken anti-rabbit Alexa Fluor™ 647, Invitrogen, A-21443, 1:1000), and incubated 30 min in dark at room temperature. Then, the cells were washed twice with PBS containing 2.5% BSA and 0.1% Triton X-100, resuspend PBS containing 2.5% BSA, and subjected to analysis using a flow cytometer (Accuri C6 plus, BD Biosciences)

Cell viability analysis

The viability of cells was analyzed using CellTiter-Glo® 2.0 Cell Viability Assay (Promega, G9241) according to the manufacturer's instructions. After incubation with the provided reagent, luminescence was measured using a plate reader (Molecular Devices; San Jose, CA, SpectraMax® iD3). The measured luminescence intensity was normalized to the intensity of the unmodified substrates (PBS) for each substrate.

Image analysis

The fluorescence intensity of laminin and live/dead cells was quantified using Fiji/ImageJ software. The mean fluorescence intensity of each image was subtracted by the mean fluorescence intensity of the background. Background-subtracted intensities from three random fields of view of each well were averaged to get a representative intensity value for each biological replicate. The three averaged intensities of the three biological replicates (three wells) were used for statistical analysis. The intensity values were normalized to the control condition (PBS, TC-treated) and presented as mean ± standard deviation. Statistical comparisons were performed using a one-way ANOVA with Tukey's post hoc test or Student's t-test (*: $p<0.05$, **: $p<0.01$). The fluorescence intensity profile of Hoechst, BRACHYURY, E-CADHERIN, CD34, and CD31 was quantified

using Fiji/ImageJ software. The intensity profile of arbitrary boxes orthogonal to the edge line of three different patterns was first analyzed. These intensity profiles were normalized and aligned based on the maximum intensity of BRACHYURY or CD34 (the maximum intensity point was set to distance 0). The intensity profiles of the markers were shown as mean (line) ± standard deviation (filled area).

3. Results

3.1 pNE-mediated surface modification for Matrigel coating

We tested the capability of pNE-coated surfaces to support hPSC culture using Matrigel as the ECM component and various substrates (TC-treated PS, untreated PS, glass, PDMS, and ULA plates) for modification. After the substrates were modified with pNE, they were washed with PBS to remove residual NE before Matrigel coating. Since laminin and type IV collagen are abundant in Matrigel, the surfaces were immunostained with an anti-laminin antibody and imaged using a fluorescence microscope to visualize the Matrigel coating (Figure 1a). Statistical differences in the fluorescence intensity of laminin immunostaining between pNE-modified and unmodified substrates were not found except the untreated PS and ULA (Figure 1b). The stronger intensity of laminin on unmodified PS is possibly due to the hydrophobic property of PS which can increase protein adsorption by hydrophobic interaction [34]. Interestingly, laminin was observed on the pNE-modified ULA surface, suggesting that pNE-mediated surface modification made the non-adhesive ULA surface favorable for Matrigel coating, likely through the covalent binding of amines and thiols in proteins to the pNE layer. Despite the ULA surface being superhydrophilic and resistant to protein adsorption, the pNE and Matrigel was successfully deposited on it, demonstrating the versatility of this surface modification.

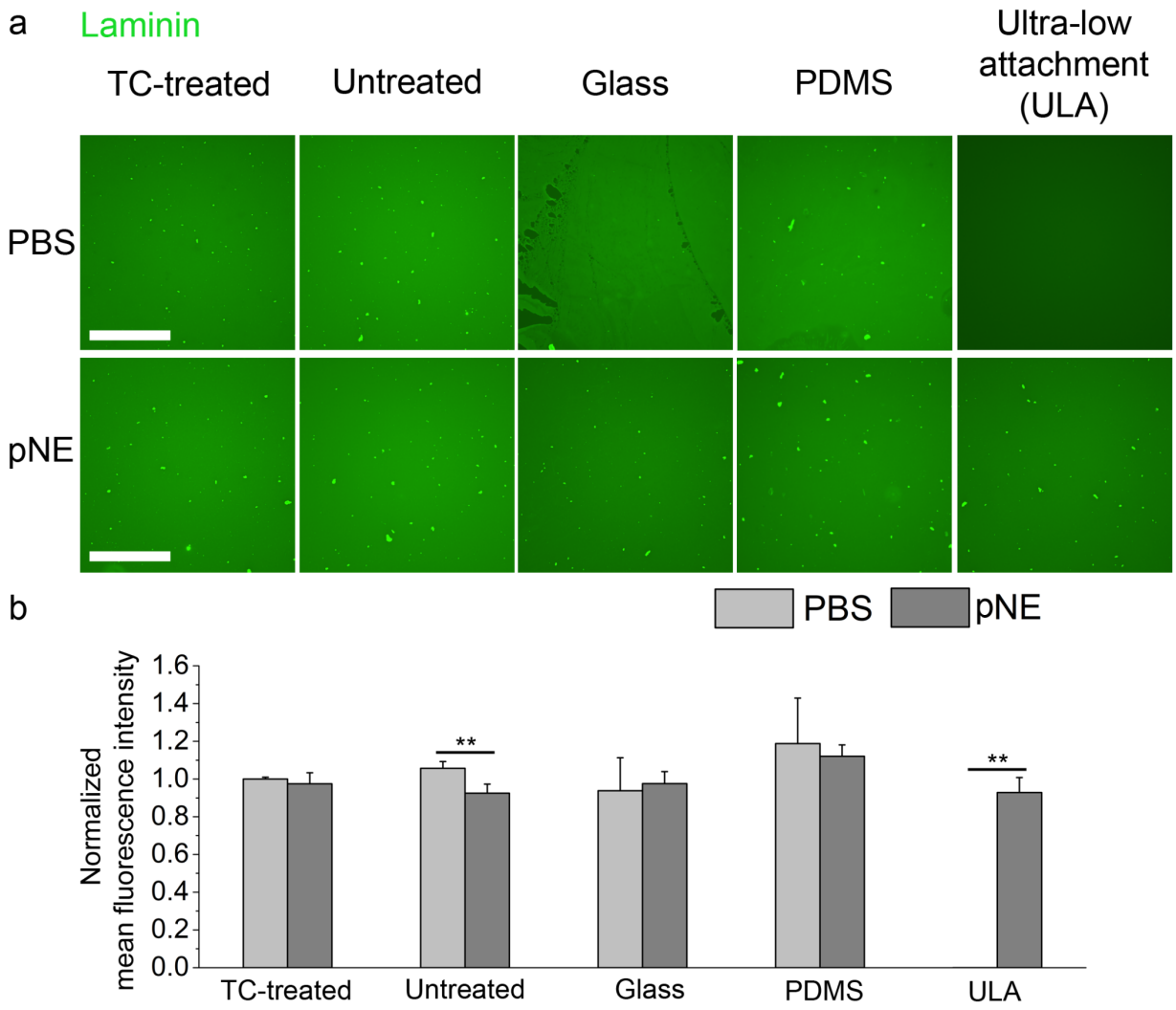

Figure 1. pNE-Mediated Surface Modification for Matrigel Coating. (a) Immunofluorescence images of laminin on either unmodified (PBS) or modified (pNE) substrates (TC-treated PS, untreated PS, glass, PDMS, and ULA surface) after Matrigel coating. Scale bars = 500 μm. (b) Quantification of fluorescence intensities of laminin. Background subtraction was performed for the mean fluorescence intensity of each image. The resulting mean intensity value was normalized to the mean intensity of the unmodified TC-treated surface (PBS, TC-treated). Statistical comparison was performed using a Student's t-test between PBS vs pNE conditions (* $p<0.05$, ** $p<0.01$, $n=3$).

3.2 pNE-mediated surface modification for hPSC culture

We next investigated the effects of pNE-mediated surface modification on hPSC culture after Matrigel coating. To test initial cell attachment, H9 hESCs were seeded at a high density (200,000 cells/cm^2), stained with live-dead cell dyes 6 hours post-seeding, and imaged using a fluorescence microscope (Figure 2a). Fluorescence intensities of the live cells on each condition were quantified and statistical comparison was performed between the unmodified (PBS) and pNE-modified (pNE) substrates (Figure 2b). Cells were not found on the unmodified ULA substrate, consistent with the lack of detectable adsorbed ECM proteins on this substrate. However, confluent hPSCs were observed on the pNE-modified ULA substrate which aligns with previous findings showing enhanced laminin immobilization on the pNE-modified ULA surface, supporting hPSC culture. Lower initial cell attachment was observed on the unmodified PDMS compared to other surfaces. The pNE coating made initial cell attachment on PDMS comparable to other pNE-modified and unmodified surfaces except the unmodified ULA. Statistical differences were not found in dead cell staining intensities among all the tested conditions except the unmodified ULA, which lacked both live and dead cells. To better quantify the cell viability, the viability of H9 hESCs 6 hours post-seeding was assessed using CellTiter-Glo® 2.0 Cell Viability Assay (Figure 2c). Due to the differences in the culture area and cell numbers in each substrate, the measured luminescence intensity of pNE-modified substrate was normalized to the intensity of the corresponding unmodified substrate (PBS). As expected, the pNE-modified ULA significantly improved the cell attachment and viability.

To evaluate the effects of pNE-modified surfaces on hPSC colony formation and sustained culture, hPSCs were singularized and seeded at a lower density (20,000 cells/cm^2), cultured for two days, stained with live-dead cell dyes, and imaged using a fluorescence microscope (Figure

2d). Fluorescence intensities of the dyes for live and dead cells were quantified and statistical comparison was performed between the unmodified (PBS) and pNE-modified (pNE) substrates (Figure 2e). As expected, no cells were observed on the unmodified ULA substrate. Very few cell colonies were found on the unmodified PDMS surface, suggesting that it has limited capability to support hPSC colony formation under the sparse and singularized condition. pNE modification enhanced hPSC colony formation and prolonged culture on PDMS and ULA substrates, though live cell fluorescence intensities on these surfaces were still lower than the other conditions. ~~those on both unmodified and pNE-modified TC-treated PS, untreated PS, and glass surfaces.~~ For both live cell intensity and viability analysis via CellTiter-Glo® 2.0 Cell Viability Assay (Figure 2c), the unmodified untreated PS showed more cells on the substrate than the pNE-modified untreated PS. It is possibly due to the hydrophobic characteristic of untreated PS facilitating ECM protein adsorption (Figure 1b) and subsequent cell attachment and growth. Like the results from the live cell intensity analysis, the pNE-modified PDMS and ULA improved cell viability after 3 days of culture.

These results demonstrate that pNE-mediated surface modification enhanced both initial hPSC attachment and colony formation, particularly on PDMS and ULA surfaces.

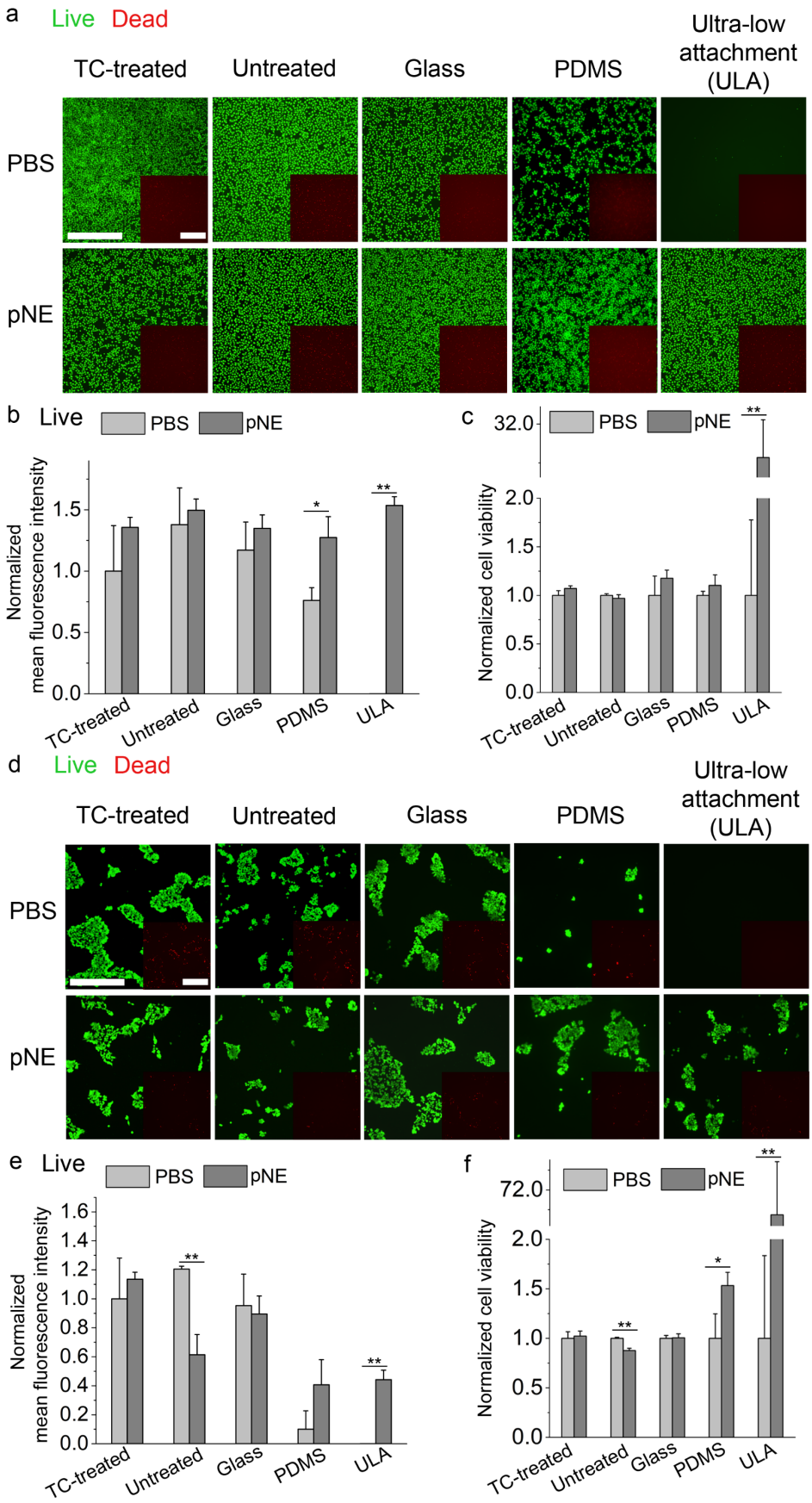
a
Live
Dead
TC-treated
Untreated
Glass
PDMS
Ultra-low attachment (ULA)
PBS
pNE
b
Live
PBS
pNE
Normalized mean fluorescence intensity
0.0
0.5
1.0
1.5
*
**
TC-treated
Untreated
Glass
PDMS
ULA
c
32.0
PBS
pNE
**
Normalized cell viability
0.0
0.5
1.0
1.5
2.0
TC-treated
Untreated
Glass
PDMS
ULA
d
Live
Dead
TC-treated
Untreated
Glass
PDMS
Ultra-low attachment (ULA)
PBS
pNE
e
Live
PBS
pNE
Normalized mean fluorescence intensity
0.0
0.2
0.4
0.6
0.8
1.0
1.2
1.4
1.6
**
**
TC-treated
Untreated
Glass
PDMS
ULA
f
72.0
PBS
pNE
**
Normalized cell viability
0.0
0.5
1.0
1.5
2.0
**
*
TC-treated
Untreated
Glass
PDMS
ULA

Figure 2. pNE-Mediated Surface Modification for hPSC Culture. (a) Fluorescence images of hPSCs seeded on either unmodified (PBS) or pNE-modified (pNE) substrates (TC-treated PS, untreated PS, glass, PDMS, and ULA surface) stained with live-dead cell dyes 6 hours after seeding (200,000 cells/cm^2). Scale bars = 500 μm. (b) Quantification of fluorescence intensities of live cell staining 6 hours after seeding. Background subtraction was performed for the mean fluorescence intensity of each image. The resulting mean intensity value was normalized to the mean intensity of the unmodified TC-treated surface (PBS, TC-treated). (c) Cell viability of hPSCs 6 hours after seeding. The measured luminescence intensity was normalized to the intensity of the unmodified substrate (PBS). (d) Fluorescence images of hPSCs on either unmodified (PBS) or pNE-modified (pNE) substrates (TC-treated PS, untreated PS, glass, PDMS, and ULA surface) stained with live-dead cell dyes 2 days after seeding (20,000 cells/cm^2). Scale bars = 500 μm. (e) Quantification of fluorescence intensities of live cell staining. Background subtraction was performed for the mean fluorescence intensity of each image. The resulting mean intensity value was normalized to the mean intensity of the unmodified TC-treated surface (PBS, TC-treated). (f) Cell viability of hPSCs 3 days after seeding. The measured luminescence intensity was normalized to the intensity of the unmodified substrate (PBS). Statistical comparison was performed using a Student's t-test between unmodified (PBS) and pNE-modified (pNE) condition (* $p<0.05$, ** $p<0.01$, $n=3$).

To assess the effects of different NE concentration on the initial cell attachment, various concentration of NE solution was tested for the surface modification of ULA and subsequent cell attachment (Figure S1). Although the reported optimal concentration of NE for surface modification is 2 mg/ml [22], wide range of NE concentration (0.2 mg/ml – 20 mg/ml) allowed the modification of ULA for the attachment of hPSCs. To better understand the initial cell attachment

process on pNE-modified substrate, hPSCs seeded on the unmodified and pNE-modified TC and ULA surface were live imaged (Movie S1, S2, S3, S4, Figure S2a, S2b). While there is no significant difference in the initial cell attachment dynamics between the unmodified and pNE-modified TC-treated PS (Figure S2a), cells were not attached to the unmodified ULA and floating around as compared to the attached cells on the pNE-modified ULA (Figure S2b). The cells on both unmodified and pNE-modified substrates were cultured for 3 more days and there is no significant difference observed in the cell density, indicating the pNE modification on TC-treated PS does not affect the initial cell attachment and growth (Figure S2c).

3.3 pNE-mediated surface modification for maintaining pluripotency

To test whether pNE-mediated surface modification can also be used to maintain pluripotency of hPSCs on various substrates, hPSCs were cultured on the unmodified and pNE-modified substrates for 4 days and analyzed for pluripotency marker expression (Figure 3). hPSCs lost some extent of pluripotency on unmodified untreated PS due to its strong hydrophobicity that can denature essential proteins for pluripotency maintenance[35]. Interestingly, hPSCs cultured on the pNE-modified untreated PS showed similar pluripotency compared to other conditions, suggesting that the pNE modification helps to maintain pluripotency of hPSCs on highly hydrophobic surfaces (Figure 3b).

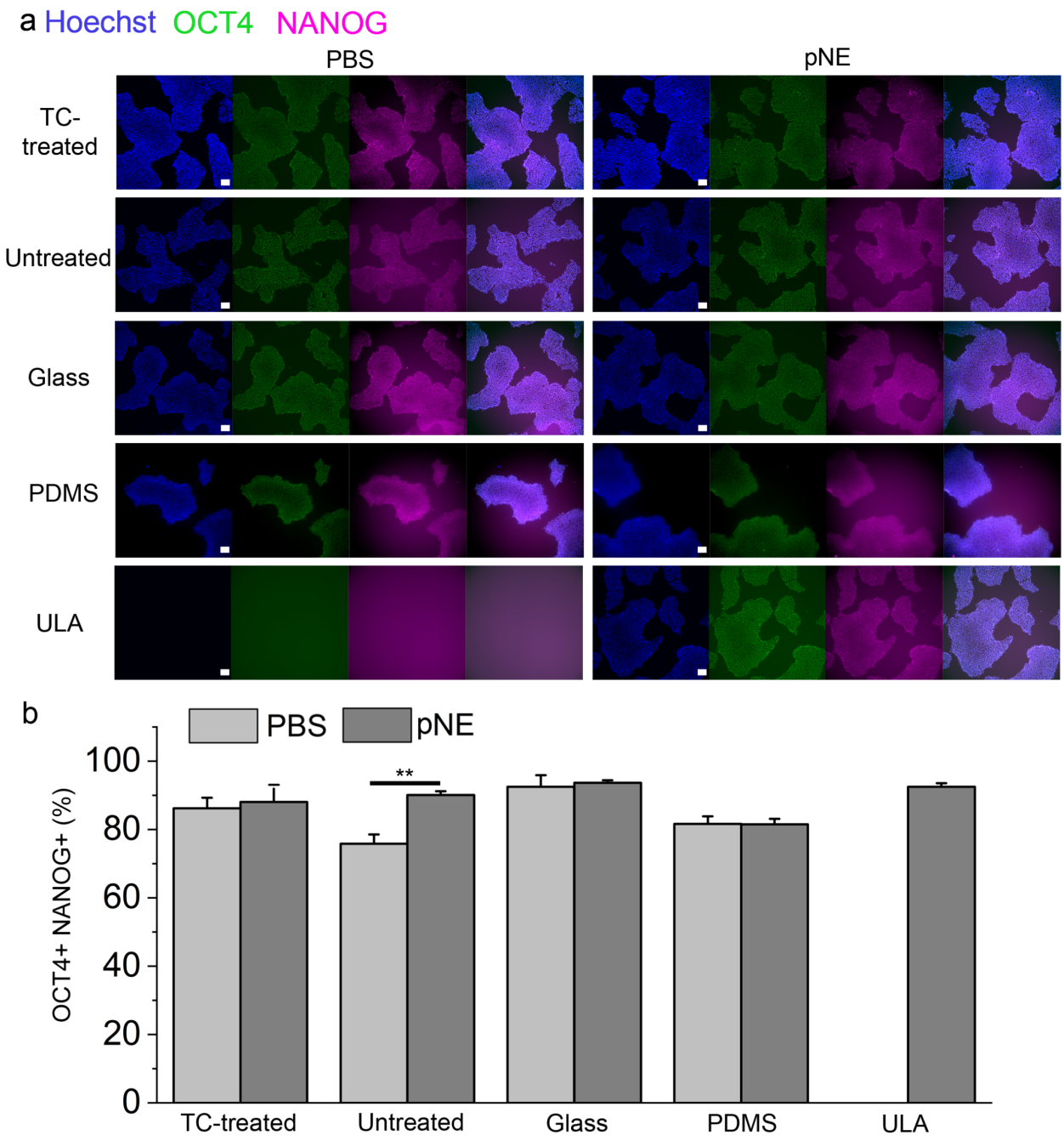

Figure 3. pNE-Mediated Surface Modification for Maintenance of Pluripotency. (a) Fluorescence images of hPSCs cultured for 4 days on unmodified or pNE-modified substrates showing the expression of pluripotency markers (OCT4, NANOG). Scale bars = 100 μm. (b) Flow cytometry analysis of hPSCs cultured for 4 days on unmodified or pNE-modified substrates showing the expression of pluripotency markers (OCT4, NANOG). Statistical comparison was performed

using a Student's t-test between unmodified (PBS) and pNE-modified (pNE) condition (* $p<0.05$, ** $p<0.01$, $n=3$).

3.4 Effects of pNE-mediated surface modification on differentiation of hPSCs

While the pNE coating enabled hPSC attachment on the ULA substrate, no significant effects of pNE modification on TC-treated surface were observed with respect to the cell attachment, growth, and pluripotency (Figure 2, Figure 3, Figure S2). To further evaluate the effects of pNE modification on their differentiation efficiency, hPSCs were differentiated into mesendoderm (Figure S3a), endothelial cells (Figure S3b), and cardiomyocytes (CMs) (Figure S3c). While there was no significant improvement in the differentiation efficiency in these three tested lineages, more consistence between biological replicates was observed on the pNE-modified surface as evidenced by the small standard deviation. This trend was also observed in the cell attachment and growth (Figure 2b, 2e). To assess the effects of pNE modification on the physiology of CMs, the differentiated CMs were stained with alpha actinin for sarcomere analysis (Figure S4a). No significant difference was observed in the expression profile of alpha actinin as well as the beating rate of CMs (Figure S4b, Movie S5, Movie S6) between PBS and pNE condition. These results might suggest that the pNE modification is beneficial to improve consistency of culture and differentiation of hPSCs, but further investigation is needed.

3.5 pNE-mediated surface modification for cell patterning

The pNE coating converted the ULA substrate from an anti-adhesive to an adhesive surface for ECM protein adsorption, allowing hPSC attachment. We hypothesized that patterning the ULA surface with pNE coating could restrict cell attachment to the patterned region, enabling cell patterning. To test this, NE solution was placed on a ULA surface as a droplet or confined with

PDMS stencil masks immediately after mixing with sodium periodate solution for NE oxidation. Live-dead cell dye staining showed that hPSCs were found only on the pNE-coated region, exhibiting patterned cell colonies (Figure 4a). Furthermore, pNE-modified ULA surfaces supported patterning of hPSC-derived cardiac progenitor cells (CPCs) in the same manner, resulting in patterned CMs on the ULA surface after culture for 7 days (Figure 4b). These results demonstrate that pNE-mediated surface modification allows spatially controlled cell patterning using pre-patterning of pNE surface modification.

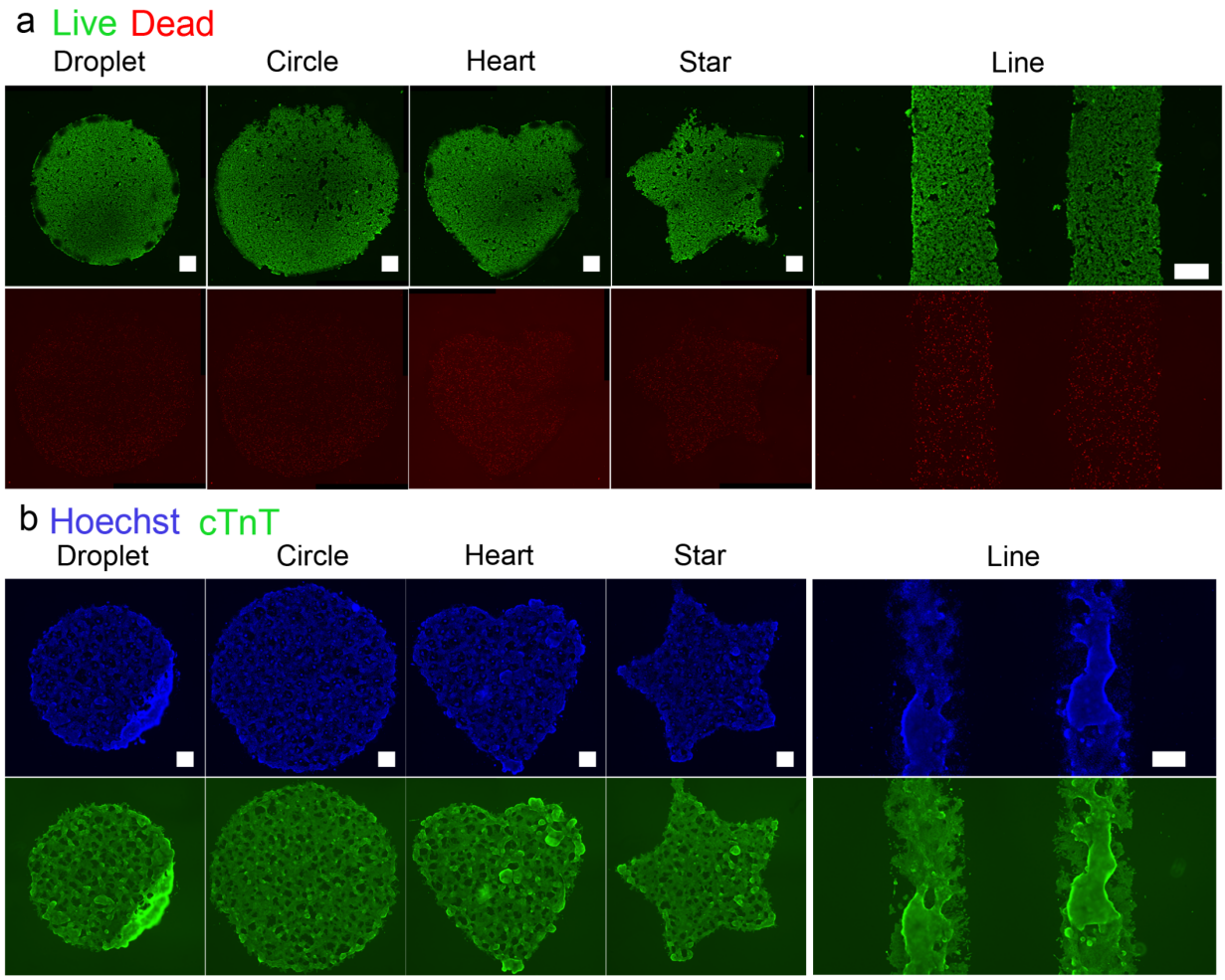

Figure 4. pNE-Mediated Surface Modification for Cell Patterning. (a) Fluorescence images of patterned hPSCs. pNE was pre-patterned using various PDMS stencil masks followed by Matrigel coating and hPSC seeding. hPSCs were stained with live-dead cell dyes one day after seeding. Scale bars = 500 μm. (b) Fluorescence images of patterned CMs. pNE was pre-patterned using various PDMS stencil masks followed by Matrigel coating and CPC seeding. CPCs were stained with cTnT and Hoechst 7 days after seeding.

3.6 Effects of cell patterning on differentiation of hPSCs

Pattern formation is crucial during human development, yet addressing this spatial event *in vitro* is challenging as typical 2D hPSC differentiation lacks spatial control over cell culture. Utilizing the spatial confinement of cells on the pNE-coated ULA surface allows cell patterning and investigating its effects on hPSC differentiation. pNE were patterned as droplet or star-shaped on ULA surface and hPSC were seeded on the pNE-modified patterns. The cells were differentiated into mesoderm lineage by treating with CHIR99021, a Wnt activator, and immunostained for BRACHYURY (BRA), a mesendoderm marker. Interestingly, BRA expression was restricted to the edges of cell patterns where cell growth was restrained by the ULA substrate (Figure 5a). BRA expression was highest within approximately 100 μm of the edge. It has been reported that BRA represses E-CADHERIN (E-CAD) expression by binding to its promoter[36]. As expected, E-CAD expression was suppressed at the periphery of cell patterns. This effect was observed regardless of macroscopic pattern shapes, even in asymmetric star pattern (Figure 5b), but not at the edges of a well where cell growth was physically blocked by the well walls (Figure 5c). When patterned hPSCs were differentiated into endothelial cells, endothelial markers CD34 and CD31, were predominantly found at the pattern periphery (Figure 6a). This phenomenon was observed in

asymmetric geometries, such as star pattern (Figure 6b). The patterned hPSCs were also further differentiated into CMs (Figure S5). Similarly, more cTnT expression were found at the pattern periphery, but cell detachment occurred due to the beating phenotype of CMs.

Symmetric patterns are typically observed in geometrically confined hPSC colonies during self-organization, but asymmetric organization is also observed during development, especially within the axis formation[37]. While the pattern formation is generally guided by morphogen gradients, it has been reported that different geometries also influence the asymmetric pattern formation of early hPSC differentiation *in vitro*[38]. The versatility of this approach in creating various geometries, both symmetric and asymmetric, may be useful for studying pattern formation with hPSCs.

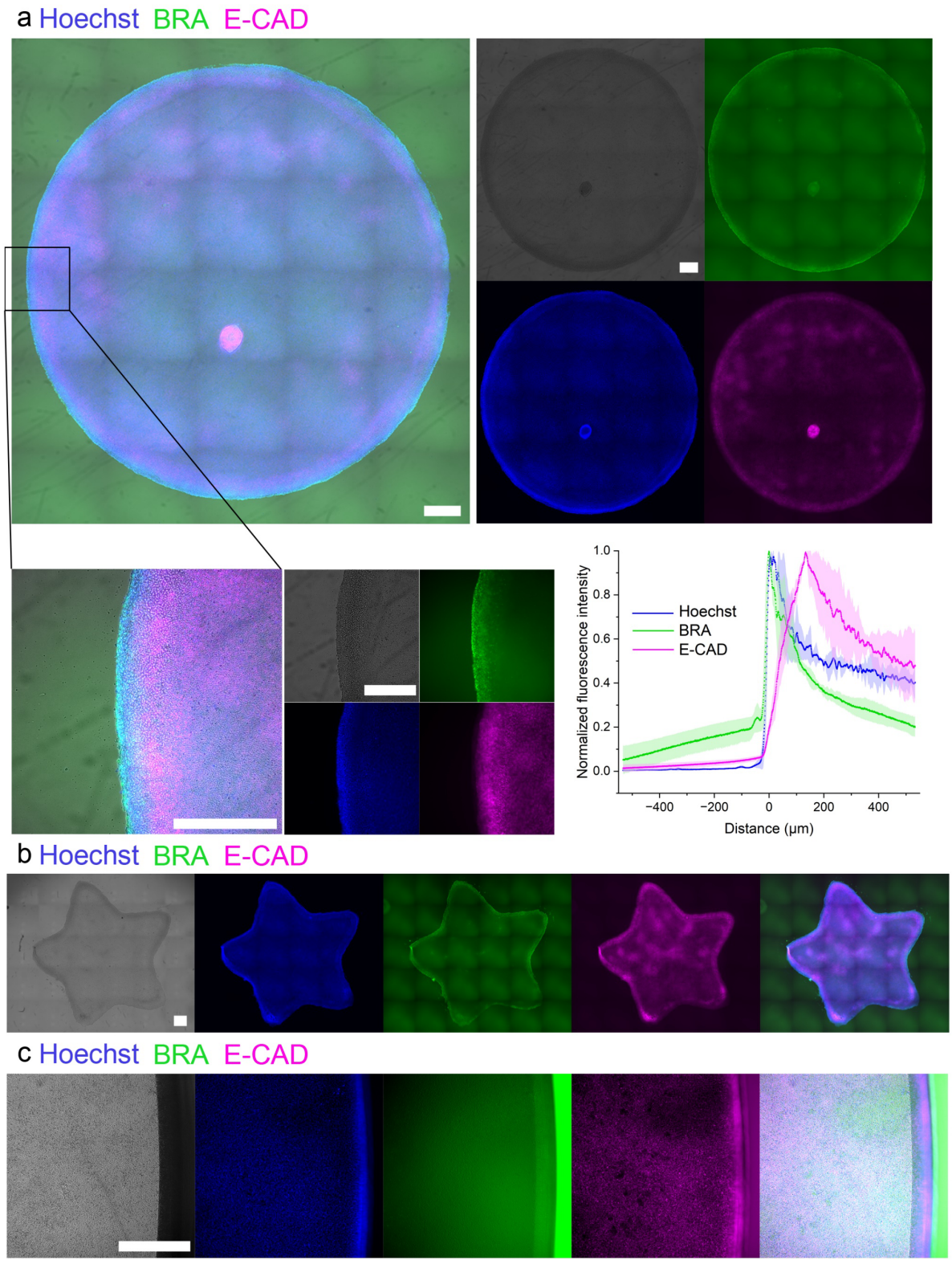
a Hoechst BRA E-CAD
Normalized fluorescence intensity
1.0
0.8
0.6
0.4
0.2
0.0
Hoechst
BRA
E-CAD
−400
−200
0
200
400
Distance (μm)
b Hoechst BRA E-CAD
c Hoechst BRA E-CAD

Figure 5. The Effects of pNE-Mediated Cell Patterning on Mesoderm Differentiation from hPSCs. (a) Fluorescence images of droplet-patterned cells. hPSCs were differentiated into mesoderm by Wnt activation on day 0. Differentiated cells were immunostained on day 2 for BRACHYURY (BRA) and E-CADHERIN (E-CAD). Expression profiles of BRA and E-CAD were analyzed with normalized fluorescence intensity. Images of three independent patterns were aligned and assessed by setting the peak expression of BRA on the x-axis as a reference point (distance 0). (b) Fluorescence images of star-patterned cells. (c) Fluorescence images of differentiated cells (day 2) at the edge of pNE-coated ULA well. Scale bars = 500 μm.

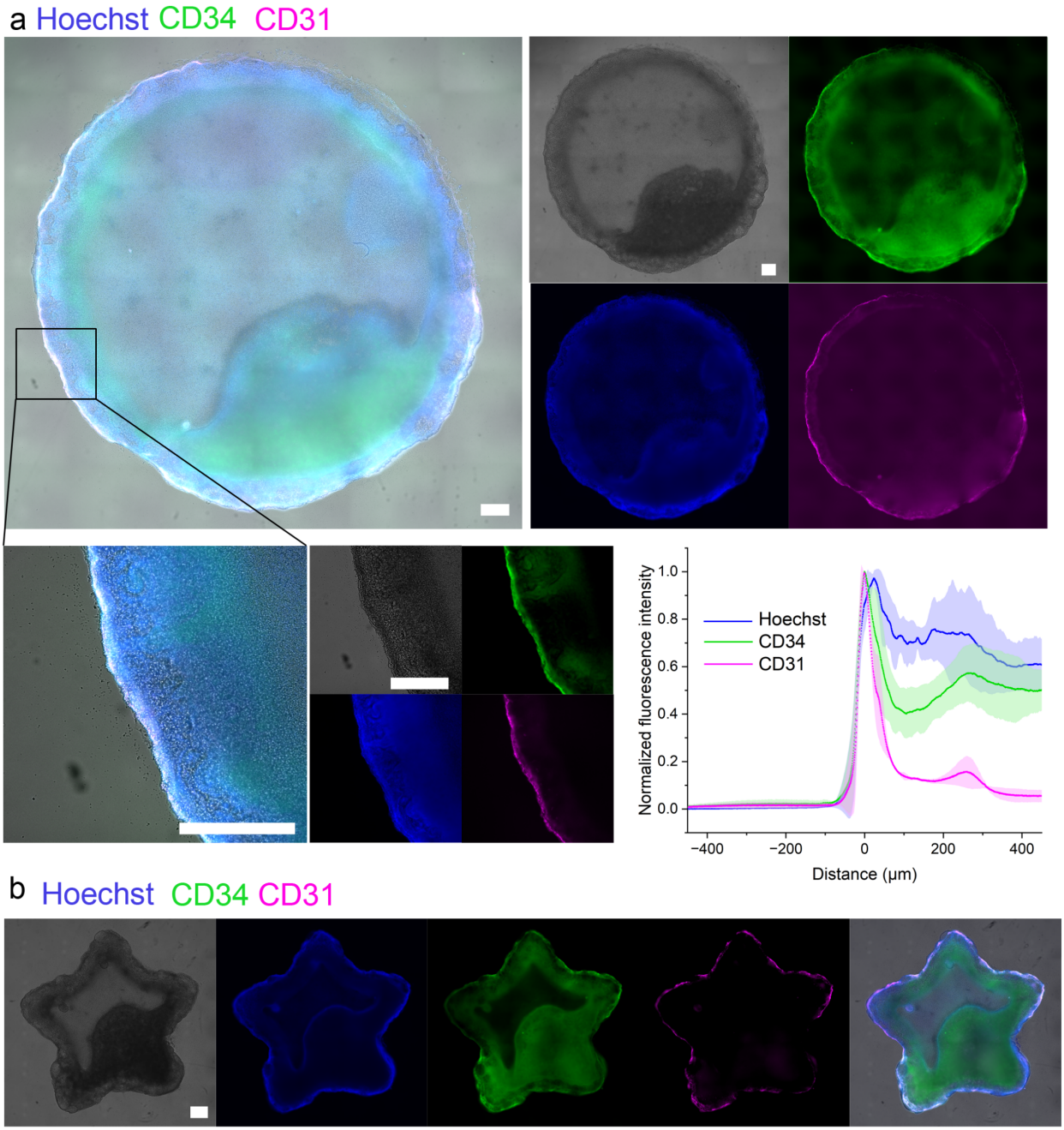

Figure 6. The effects of pNE-Mediated Cell Patterning on Endothelial Cell Differentiation from hPSCs. (a) Fluorescence images of droplet-patterned cells. hPSCs were differentiated into endothelial cells by Wnt activation on day 0 and subsequent treatment with VEGF from day 2. Differentiated cells were immunostained on day 4 for CD34 and CD31. Expression profiles of CD34 and CD31 were analyzed with normalized fluorescence intensity. Images of three

independent patterns were aligned and assessed by setting the peak expression of CD34 on the x-axis as a reference point (distance 0). (b) Fluorescence images of star-patterned cells. Scale bars = 500 μm.

4. Discussion

In this study, we presented a surface modification strategy using pNE coating for hPSC culture and differentiation on substrates not previously amenable to ECM protein adsorption, thus fail to support cell attachment or maintain pluripotency. We also demonstrated that this strategy can be used for cell patterning when pNE is pre-patterned on a non-adhesive substrate followed by ECM coating.

Poly(catecholamine) materials like poly(dopamine) (pDA) and pNE have been extensively studied for substrate-independent surface modification, enabling the immobilization and delivery of bioactive molecules such as peptides[28], growth factors[39], polysaccharides[40], and viruses[41]. Immobilization of peptides and ECM proteins for hPSC culture on pDA-coated substrates has been reported[28–32], but the use of pNE coating on ULA surfaces for hPSC culture had not been previously reported.

Our findings indicate that pNE coating effectively modifies ULA substrates for enhanced ECM protein immobilization, facilitating hPSC attachment and growth. Unlike TC-treated PS, untreated PS, and glass, the unmodified PDMS substrate showed significantly lower initial cell attachment and hPSC colony formation after two days of culture, while pNE-modified PDMS showed increased cell attachment and growth. Although significant difference was not detected in laminin staining between PDMS and other substrates, the overall amount of ECM proteins on the PDMS substrate may differ between the unmodified and pNE-modified conditions as Matrigel contains

other ECM proteins such as collagen. PDMS is widely used in microfluidic device construction due to its biocompatibility, optical transparency, and ease of fabrication[42]. However, its high hydrophobicity, which is not optimal for cell adhesion and growth, necessitates surface modification strategies for its use in microfluidic technology[43]. pDA-mediated surface modification of PDMS has been shown to improve cell adhesion and growth[44,45] and promote ECM protein deposition for cell culture[27,46]. Our study demonstrated that pNE coating on PDMS enhances initial hPSC attachment and subsequent colony formation, consistent with previous studies. pNE coating is suggested to enhance ECM protein immobilization via covalent conjugation between proteins and the pNE film. Additionally, pNE can render substrates more hydrophilic due to the presence of hydroxyl groups and secondary amines[44,45], further aiding protein adsorption to the modified surface. This was also demonstrated by the improved pluripotency of hPSCs cultured on the pNE-modified untreated PS surface compared to the hPSCs cultured on the unmodified hydrophobic PS. While there was no significant improvement in cell attachment, growth, and differentiation efficiency of hPSCs on pNE-modified TC-treated substrate compared to the unmodified surface, some of the results possibly indicate that the pNE modification may be helpful to achieve homogeneity of cellular outcomes.

We utilized the non-adhesive property of the ULA surface along with pNE coating to achieve cell patterning. Spatial patterning of hPSCs can be used to study the effects of asymmetrical confinement on hPSC colonies, addressing issues such as cell fate heterogeneity and spatial cell polarization[38,47–49]. PDMS stencil masks with various shapes were used to confine NE solutions to specific parts of the ULA surface, resulting in patterned hPSCs. The ULA surface prevents attachment of cell-secreted ECM proteins to unmodified areas, making studies of spatial effects on hPSC fate or differentiation more feasible with this simple pNE-ULA cell patterning method.

Indeed, patterned cells on ULA were differentiated into mesendoderm, and spatial heterogeneity of differentiated cells was evaluated. On day 2, BRA expression was restricted to the pattern periphery, consistent with previous reports where differentiated hPSCs from micropatterned colonies showed localized BRA expression at the colony periphery[48]. This study suggested that areas with elevated integrin adhesion-mediated contractile stresses, such as colony edges, have activated myosin II localized to the actomyosin contractile cable rather than the E-CAD adherens junction network, resulting in mesendoderm differentiation. When localized mesoderm was further differentiated into endothelial cells and CMs, the cell fate profile was maintained, indicated by CD34, CD31, and cTnT expression at the pattern periphery.

We also demonstrated that CMs can be patterned directly from hPSCs and from hPSC-derived CPCs. Previous studies have reported that the geometries of hPSC colonies influence the generation of patterned cardiac organoids[50,51]. Additionally, the width of rectangular micropatterns has been shown to affect the cell alignment and sarcomere formation of hPSC-derived CMs[52]. Our pNE-mediated surface modification approach could offer a simple method to investigate the effects of spatial patterning on CM function and physiology. It is noteworthy that NE, as a neurotransmitter, plays a significant role in CM physiology[53]. NE released by neurons modulates CM electrophysiology and excessive NE concentration may be involved in cardiovascular diseases[54]. While we expect no residual NE after substrate modification, as NE undergoes active oxidation and tautomerization to form a polymerized form[22] and the limited analysis on CM physiology on unmodified and pNE-modified substrate suggested no significant change in the characteristics of these CMs, additional verification is needed to evaluate the effects of pNE-modified substrates on CM physiology.

5. Conclusions

Overall, pNE-mediated surface modification enables hPSC culture and differentiation on various materials not previously suitable for hPSC culture in a simple and versatile manner. This technique provides opportunities to study the effects of different surface properties on hPSC physiology and the application of hPSCs in various tissue engineering constructs. Additionally, with non-adhesive substrates, pNE coating allows easy cell patterning to study aspects of cellular functions, including differentiation, in a spatially controlled context.

Acknowledgments

We are grateful for the support from the American Heart Association (Postdoctoral Fellowship (grant no. 23POST1025924 to G.J.), NIH (NIH NCI (grant no. R37CA265926 to X.B.)), and NSF (NSF CBET (grant no. 2143064 to X.B.)). We also thank you all the members of the Palecek and Bao lab.

Author Contributions

G.J. conceived, designed, and performed the experiments. H.H. assisted in data collection and analysis. G.J., X.B., and S.P. wrote the manuscript.

References

(1) Chen, K. G.; Mallon, B. S.; McKay, R. D. G.; Robey, P. G. Human Pluripotent Stem Cell Culture: Considerations for Maintenance, Expansion, and Therapeutics. *Cell Stem Cell*. 2014. https://doi.org/10.1016/j.stem.2013.12.005.

(2) Aisenbrey, E. A.; Murphy, W. L. Synthetic Alternatives to Matrigel. *Nature Reviews Materials*. 2020. https://doi.org/10.1038/s41578-020-0199-8.

(3) Thomson, J. A. Embryonic Stem Cell Lines Derived from Human Blastocysts. *Science (1979)* **1998**, *282* (5391). https://doi.org/10.1126/science.282.5391.1145.

(4) Xu, C.; Inokuma, M. S.; Denham, J.; Golds, K.; Kundu, P.; Gold, J. D.; Carpenter, M. K. Feeder-Free Growth of Undifferentiated Human Embryonic Stem Cells. *Nat Biotechnol* **2001**, *19* (10). https://doi.org/10.1038/nbt1001-971.

(5) Braam, S. R.; Zeinstra, L.; Litjens, S.; Ward-van Oostwaard, D.; van den Brink, S.; van Laake, L.; Lebrin, F.; Kats, P.; Hochstenbach, R.; Passier, R.; Sonnenberg, A.; Mummery, C. L. Recombinant Vitronectin Is a Functionally Defined Substrate That Supports Human Embryonic Stem Cell Self-Renewal via AVβ5 Integrin. *Stem Cells* **2008**, *26* (9). https://doi.org/10.1634/stemcells.2008-0291.

(6) Rodin, S.; Domogatskaya, A.; Ström, S.; Hansson, E. M.; Chien, K. R.; Inzunza, J.; Hovatta, O.; Tryggvason, K. Long-Term Self-Renewal of Human Pluripotent Stem Cells on Human Recombinant Laminin-511. *Nat Biotechnol* **2010**, *28* (6). https://doi.org/10.1038/nbt.1620.

(7) Brafman, D. A.; Chang, C. W.; Fernandez, A.; Willert, K.; Varghese, S.; Chien, S. Long-Term Human Pluripotent Stem Cell Self-Renewal on Synthetic Polymer Surfaces. *Biomaterials* **2010**, *31* (34). https://doi.org/10.1016/j.biomaterials.2010.08.007.

(8) Klim, J. R.; Li, L.; Wrighton, P. J.; Piekarczyk, M. S.; Kiessling, L. L. A Defined Glycosaminoglycan-Binding Substratum for Human Pluripotent Stem Cells. *Nat Methods* **2010**, *7* (12). https://doi.org/10.1038/nmeth.1532.

(9) Melkoumian, Z.; Weber, J. L.; Weber, D. M.; Fadeev, A. G.; Zhou, Y.; Dolley-Sonneville, P.; Yang, J.; Qiu, L.; Priest, C. A.; Shogbon, C.; Martin, A. W.; Nelson, J.; West, P.; Beltzer, J. P.; Pal, S.; Brandenberger, R. Synthetic Peptide-Acrylate Surfaces for Long-Term Self-Renewal and Cardiomyocyte Differentiation of Human Embryonic Stem Cells. *Nat Biotechnol* **2010**, *28* (6). https://doi.org/10.1038/nbt.1629.

(10) Mei, Y.; Saha, K.; Bogatyrev, S. R.; Yang, J.; Hook, A. L.; Kalcioglu, Z. I.; Cho, S. W.; Mitalipova, M.; Pyzocha, N.; Rojas, F.; Van Vliet, K. J.; Davies, M. C.; Alexander, M. R.; Langer, R.; Jaenisch, R.; Anderson, D. G. Combinatorial Development of Biomaterials for Clonal Growth of Human Pluripotent Stem Cells. *Nat Mater* **2010**, *9* (9). https://doi.org/10.1038/nmat2812.

(11) Nandivada, H.; Villa-Diaz, L. G.; O'Shea, K. S.; Smith, G. D.; Krebsbach, P. H.; Lahann, J. Fabrication of Synthetic Polymer Coatings and Their Use in Feeder-Free Culture of Human Embryonic Stem Cells. *Nat Protoc* **2011**, *6* (7). https://doi.org/10.1038/nprot.2011.342.

(12) Villa-Diaz, L. G.; Ross, A. M.; Lahann, J.; Krebsbach, P. H. Concise Review: The Evolution of Human Pluripotent Stem Cell Culture: From Feeder Cells to Synthetic Coatings. *Stem Cells*. 2013. https://doi.org/10.1002/stem.1260.

(13) Liu, L.; Kamei, K. ichiro; Yoshioka, M.; Nakajima, M.; Li, J.; Fujimoto, N.; Terada, S.; Tokunaga, Y.; Koyama, Y.; Sato, H.; Hasegawa, K.; Nakatsuji, N.; Chen, Y. Nano-on-Micro Fibrous Extracellular Matrices for Scalable Expansion of Human ES/IPS Cells. *Biomaterials* **2017**, *124*. https://doi.org/10.1016/j.biomaterials.2017.01.039.

(14) Ji, J.; Tong, X.; Huang, X.; Wang, T.; Lin, Z.; Cao, Y.; Zhang, J.; Dong, L.; Qin, H.; Hu, Q. Sphere-Shaped Nano-Hydroxyapatite/Chitosan/Gelatin 3D Porous Scaffolds Increase Proliferation and Osteogenic Differentiation of Human Induced Pluripotent Stem Cells from Gingival Fibroblasts. *Biomedical Materials (Bristol)* **2015**, *10* (4). https://doi.org/10.1088/1748-6041/10/4/045005.

(15) Yan, Y.; Martin, L. M.; Bosco, D. B.; Bundy, J. L.; Nowakowski, R. S.; Sang, Q. X. A.; Li, Y. Differential Effects of Acellular Embryonic Matrices on Pluripotent Stem Cell Expansion and Neural Differentiation. *Biomaterials* **2015**, *73*. https://doi.org/10.1016/j.biomaterials.2015.09.020.

(16) Ovadia, E. M.; Colby, D. W.; Kloxin, A. M. Designing Well-Defined Photopolymerized Synthetic Matrices for Three-Dimensional Culture and Differentiation of Induced Pluripotent Stem Cells. *Biomater Sci* **2018**, *6* (6). https://doi.org/10.1039/c8bm00099a.

(17) Deng, Y.; Wei, S.; Yang, L.; Yang, W.; Dargusch, M. S.; Chen, Z. G. A Novel Hydrogel Surface Grafted With Dual Functional Peptides for Sustaining Long-Term Self-Renewal of Human Induced Pluripotent Stem Cells and Manipulating Their Osteoblastic Maturation. *Adv Funct Mater* **2018**, *28* (11). https://doi.org/10.1002/adfm.201705546.

(18) Deng, Y.; Yang, Y.; Wei, S. Peptide-Decorated Nanofibrous Niche Augments In Vitro Directed Osteogenic Conversion of Human Pluripotent Stem Cells. *Biomacromolecules* **2017**, *18* (2). https://doi.org/10.1021/acs.biomac.6b01748.

(19) Lee, H.; Dellatore, S. M.; Miller, W. M.; Messersmith, P. B. Mussel-Inspired Surface Chemistry for Multifunctional Coatings. *Science (1979)* **2007**, *318* (5849). https://doi.org/10.1126/science.1147241.

(20) Sung, M. K.; Rho, J.; Choi, I. S.; Messersmith, P. B.; Lee, H. Norepinephrine: Material-Independent, Multifunctional Surface Modification Reagent. *J Am Chem Soc* **2009**, *131* (37). https://doi.org/10.1021/ja905183k.

(21) Hong, S.; Na, Y. S.; Choi, S.; Song, I. T.; Kim, W. Y.; Lee, H. Non-Covalent Self-Assembly and Covalent Polymerization Co-Contribute to Polydopamine Formation. *Adv Funct Mater* **2012**, *22* (22). https://doi.org/10.1002/adfm.201201156.

(22) Hong, S.; Kim, J.; Na, Y. S.; Park, J.; Kim, S.; Singha, K.; Im, G. Il; Han, D. K.; Kim, W. J.; Lee, H. Poly(Norepinephrine): Ultrasmooth Material-Independent Surface Chemistry and Nanodepot for Nitric Oxide. *Angewandte Chemie - International Edition* **2013**, *52* (35). https://doi.org/10.1002/anie.201301646.

(23) Lee, H.; Rho, J.; Messersmith, P. B. Facile Conjugation of Biomolecules onto Surfaces via Mussel Adhesive Protein Inspired Coatings. *Adv Mater* **2009**, *21* (4), 431.

(24) Yu, X.; Walsh, J.; Wei, M. Covalent Immobilization of Collagen on Titanium through Polydopamine Coating to Improve Cellular Performances of MC3T3-E1 Cells. *RSC Adv* **2014**, *4* (14). https://doi.org/10.1039/c3ra44137g.

(25) Tapsir, Z.; Jamaludin, F. H.; Pingguan-Murphy, B.; Saidin, S. Immobilisation of Hydroxyapatite-Collagen on Polydopamine Grafted Stainless Steel 316L: Coating Adhesion and in Vitro Cells Evaluation. *J Biomater Appl* **2018**, *32* (7). https://doi.org/10.1177/0885328217744081.

(26) Teixeira, B. N.; Aprile, P.; Mendonça, R. H.; Kelly, D. J.; Thiré, R. M. da S. M. Evaluation of Bone Marrow Stem Cell Response to PLA Scaffolds Manufactured by 3D Printing and Coated with Polydopamine and Type I Collagen. *J Biomed Mater Res B Appl Biomater* **2019**, *107* (1). https://doi.org/10.1002/jbm.b.34093.

(27) Dabaghi, M.; Shahriari, S.; Saraei, N.; Da, K.; Chandiramohan, A.; Selvaganapathy, P. R.; Hirota, J. A. Article Surface Modification of Pdms-Based Microfluidic Devices with Collagen Using Polydopamine as a Spacer to Enhance Primary Human Bronchial Epithelial Cell Adhesion. *Micromachines (Basel)* **2021**, *12* (2). https://doi.org/10.3390/mi12020132.

(28) Park, H. J.; Yang, K.; Kim, M. J.; Jang, J.; Lee, M.; Kim, D. W.; Lee, H.; Cho, S. W. Bio-Inspired Oligovitronectin-Grafted Surface for Enhanced Self-Renewal and Long-Term Maintenance of Human Pluripotent Stem Cells under Feeder-Free Conditions. *Biomaterials* **2015**, *50* (1). https://doi.org/10.1016/j.biomaterials.2015.01.015.

(29) Wang, M.; Deng, Y.; Zhou, P.; Luo, Z.; Li, Q.; Xie, B.; Zhang, X.; Chen, T.; Pei, D.; Tang, Z.; Wei, S. In Vitro Culture and Directed Osteogenic Differentiation of Human Pluripotent Stem Cells on Peptides-Decorated Two-Dimensional Microenvironment. *ACS Appl Mater Interfaces* **2015**, *7* (8). https://doi.org/10.1021/acsami.5b00188.

(30) Zhou, P.; Wu, F.; Zhou, T.; Cai, X.; Zhang, S.; Zhang, X.; Li, Q.; Li, Y.; Zheng, Y.; Wang, M.; Lan, F.; Pan, G.; Pei, D.; Wei, S. Simple and Versatile Synthetic Polydopamine-Based Surface Supports Reprogramming of Human Somatic Cells and Long-Term Self-Renewal of Human Pluripotent Stem Cells under Defined Conditions. *Biomaterials* **2016**, *87*. https://doi.org/10.1016/j.biomaterials.2016.02.012.

(31) Zhou, P.; Yin, B.; Zhang, R.; Xu, Z.; Liu, Y.; Yan, Y.; Zhang, X.; Zhang, S.; Li, Y.; Liu, H.; Yuan, Y. A.; Wei, S. Molecular Basis for RGD-Containing Peptides Supporting Adhesion and Self-Renewal of Human Pluripotent Stem Cells on Synthetic Surface. *Colloids Surf B Biointerfaces* **2018**, *171*. https://doi.org/10.1016/j.colsurfb.2018.07.050.

(32) Lee, M.; Kim, Y.; Ryu, J. H.; Kim, K.; Han, Y. M.; Lee, H. Long-Term, Feeder-Free Maintenance of Human Embryonic Stem Cells by Mussel-Inspired Adhesive Heparin and Collagen Type I. *Acta Biomater* **2016**, *32*. https://doi.org/10.1016/j.actbio.2016.01.008.

(33) Lian, X.; Hsiao, C.; Wilson, G.; Zhu, K.; Hazeltine, L. B.; Azarin, S. M.; Raval, K. K.; Zhang, J.; Kamp, T. J.; Palecek, S. P. Robust Cardiomyocyte Differentiation from Human Pluripotent Stem Cells via Temporal Modulation of Canonical Wnt Signaling. *Proc Natl Acad Sci U S A* **2012**, *109* (27). https://doi.org/10.1073/pnas.1200250109.

(34) Malmsten, M. Ellipsometry Studies of the Effects of Surface Hydrophobicity on Protein Adsorption. *Colloids Surf B Biointerfaces* **1995**, *3* (5), 297–308.

(35) Sharma, S.; Berne, B. J.; Kumar, S. K. Thermal and Structural Stability of Adsorbed Proteins. *Biophys J* **2010**, *99* (4), 1157–1165.

(36) Sun, S.; Sun, W.; Xia, L.; Liu, L.; Du, R.; He, L.; Li, R.; Wang, H.; Huang, C. The T-Box Transcription Factor Brachyury Promotes Renal Interstitial Fibrosis by Repressing E-Cadherin Expression. *Cell Communication and Signaling* **2014**, *12* (1). https://doi.org/10.1186/s12964-014-0076-4.

(37) Manfrin, A.; Tabata, Y.; Paquet, E. R.; Vuaridel, A. R.; Rivest, F. R.; Naef, F.; Lutolf, M. P. Engineered Signaling Centers for the Spatially Controlled Patterning of Human Pluripotent Stem Cells. *Nat Methods* **2019**, *16* (7). https://doi.org/10.1038/s41592-019-0455-2.

(38) Blin, G.; Wisniewski, D.; Picart, C.; Thery, M.; Puceat, M.; Lowell, S. Geometrical Confinement Controls the Asymmetric Patterning of Brachyury in Cultures of Pluripotent Cells. *Development (Cambridge)* **2018**, *145* (18). https://doi.org/10.1242/dev.166025.

(39) Yang, K.; Lee, J. S.; Kim, J.; Lee, Y. Bin; Shin, H.; Um, S. H.; Kim, J. B.; Park, K. I.; Lee, H.; Cho, S. W. Polydopamine-Mediated Surface Modification of Scaffold Materials for Human Neural Stem Cell Engineering. *Biomaterials* **2012**, *33* (29). https://doi.org/10.1016/j.biomaterials.2012.06.067.

(40) Yuan, S.; Li, Z.; Zhao, J.; Luan, S.; Ma, J.; Song, L.; Shi, H.; Jin, J.; Yin, J. Enhanced Biocompatibility of Biostable Poly(Styrene-b-Isobutylene-b- Styrene) Elastomer via Poly(Dopamine)-Assisted Chitosan/Hyaluronic Acid Immobilization. *RSC Adv* **2014**, *4* (59). https://doi.org/10.1039/c4ra04523h.

(41) Kim, E.; Lee, S.; Hong, S.; Jin, G.; Kim, M.; Park, K. I.; Lee, H.; Jang, J. H. Sticky "Delivering-from" Strategies Using Viral Vectors for Efficient Human Neural Stem Cell Infection by Bioinspired Catecholamines. *ACS Appl Mater Interfaces* **2014**, *6* (11). https://doi.org/10.1021/am5011095.

(42) McDonald, J. C.; Whitesides, G. M. Poly(Dimethylsiloxane) as a Material for Fabricating Microfluidic Devices. *Acc Chem Res* **2002**, *35* (7). https://doi.org/10.1021/ar010110q.

(43) Gokaltun, A.; Yarmush, M. L.; Asatekin, A.; Usta, O. B. Recent Advances in Nonbiofouling PDMS Surface Modification Strategies Applicable to Microfluidic Technology. *Technology (Singap World Sci)* **2017**, *05* (01). https://doi.org/10.1142/s2339547817300013.

(44) Chuah, Y. J.; Koh, Y. T.; Lim, K.; Menon, N. V.; Wu, Y.; Kang, Y. Simple Surface Engineering of Polydimethylsiloxane with Polydopamine for Stabilized Mesenchymal Stem Cell Adhesion and Multipotency. *Sci Rep* **2015**, *5*. https://doi.org/10.1038/srep18162.

(45) Park, M.; Shin, M.; Kim, E.; Lee, S.; Park, K. I.; Lee, H.; Jang, J. H. The Promotion of Human Neural Stem Cells Adhesion Using Bioinspired Poly(Norepinephrine) Nanoscale Coating. *J Nanomater* **2014**, *2014*. https://doi.org/10.1155/2014/793052.

(46) Park, S. E.; Georgescu, A.; Oh, J. M.; Kwon, K. W.; Huh, D. Polydopamine-Based Interfacial Engineering of Extracellular Matrix Hydrogels for the Construction and Long-Term Maintenance of Living Three-Dimensional Tissues. *ACS Appl Mater Interfaces* **2019**, *11* (27). https://doi.org/10.1021/acsami.9b07912.

(47) Smith, Q.; Rochman, N.; Carmo, A. M.; Vig, D.; Chan, X. Y.; Sun, S.; Gerecht, S. Cytoskeletal Tension Regulates Mesodermal Spatial Organization and Subsequent Vascular Fate. *Proc Natl Acad Sci U S A* **2018**, *115* (32). https://doi.org/10.1073/pnas.1808021115.

(48) Toh, Y. C.; Xing, J.; Yu, H. Modulation of Integrin and E-Cadherin-Mediated Adhesions to Spatially Control Heterogeneity in Human Pluripotent Stem Cell Differentiation. *Biomaterials* **2015**, *50* (1). https://doi.org/10.1016/j.biomaterials.2015.01.019.

(49) Jin, G.; Floy, M. E.; Simmons, A. D.; Arthur, M. M.; Palecek, S. P. Spatial Stem Cell Fate Engineering via Facile Morphogen Localization. *Adv Healthc Mater* **2021**, *10* (21). https://doi.org/10.1002/adhm.202100995.

(50) Ma, Z.; Wang, J.; Loskill, P.; Huebsch, N.; Koo, S.; Svedlund, F. L.; Marks, N. C.; Hua, E. W.; Grigoropoulos, C. P.; Conklin, B. R.; Healy, K. E. Self-Organizing Human Cardiac Microchambers Mediated by Geometric Confinement. *Nat Commun* **2015**, *6*. https://doi.org/10.1038/ncomms8413.

(51) Hoang, P.; Wang, J.; Conklin, B. R.; Healy, K. E.; Ma, Z. Generation of Spatial-Patterned Early-Developing Cardiac Organoids Using Human Pluripotent Stem Cells. *Nat Protoc* **2018**, *13* (4). https://doi.org/10.1038/nprot.2018.006.

(52) Salick, M. R.; Napiwocki, B. N.; Sha, J.; Knight, G. T.; Chindhy, S. A.; Kamp, T. J.; Ashton, R. S.; Crone, W. C. Micropattern Width Dependent Sarcomere Development in Human ESC-Derived Cardiomyocytes. *Biomaterials* **2014**, *35* (15). https://doi.org/10.1016/j.biomaterials.2014.02.001.

(53) Franzoso, M.; Zaglia, T.; Mongillo, M. Putting Together the Clues of the Everlasting Neuro-Cardiac Liaison. *Biochim Biophys Acta Mol Cell Res* **2016**, *1863* (7). https://doi.org/10.1016/j.bbamcr.2016.01.009.

(54) Schroeder, C.; Jordan, J. Norepinephrine Transporter Function and Human Cardiovascular Disease. *American Journal of Physiology - Heart and Circulatory Physiology*. 2012. https://doi.org/10.1152/ajpheart.00492.2012.